Northumbria Research Link

University**Library**

Semi Valley Switching for Buck LED Driver in Current Control Mode
(Jul. 2019)

Abstract—**Valley switching is one of the most efficient methods to decrease the switching losses in DC/DC converters. It uses the resonance between the converter inductance and parasitic output capacitance of MOSFET. In spite of enhancing the system efficiency, it may malfunction the converters performance. In this paper, the drawbacks of valley switching in Buck LED drivers are investigated. It shows that this method not only cause current fluctuation in Boost power factor correction converters as studied in the previous researches but also can malfunction Buck LED drivers' performance in dimming or thermal management conditions. In this study, a semi valley switching and its implementation are introduced to solve this problem. With the proposed method, it is shown that a balance between low current and switching losses is required to achieve efficient performance of Buck LED drivers in dimming or thermal management. The methodologies are implemented in an experimental prototype to verify and validate the proposed method.**

Index Terms—**Buck LED driver, current control, dimming, frequency limitation, resonance, semi valley switching.**

I. INTRODUCTION

NOWADAYS LED lamps are used extensively instead of incandescent or florescent lamps due to their long lifespan, high efficiency, and non-mercury content. On the downside, an LED lamp requires a DC/DC converter to produce constant current, thus a lot of converter topologies are introduced to enhance their performance quality and to improve their merits. These converters have poor power factor due to use of rectifier and capacitor as an output filter therefore researchers investigated the methods to decrease the overall price by designing circuits which simultaneously fulfill the roles of DC/DC converter and power factor correction (PFC) [1], [2]. On the other hand, electrolytic capacitors decrease the reliability of the LED drivers as they are eliminated in recent studies to enhance the reliability of the LED drivers [3], [4]. One of the most important aspects of all power electronic applications is their switching performance and their efficiency. An incorrect switching pattern causes some problems like chaotic phenomena in their responses [5], [6]. However, a proper switching method can decrease the switching losses and enhance the efficiency. Efficiency and power loss analyses of Buck-Flyback LED drivers were conducted in [7], which can be extended for other types of LED drivers. Some researchers used resonance circuits to increase the efficiency of LED drivers in which power switches work on zero voltage and/or zero current switching [8], [9]. One of the most popular methods in using resonance to enhance the efficiency of an LED driver is the valley switching method [10]–[12]. The valley switching uses resonance between parasitic capacitance of power switch and inductance of the converter therefore it does not require any extra elements. However, using this method may deteriorate the operation of a system as the study in [13] shows it increases the total harmonic distortion (THD) of input currents in power factor correction converters especially when the input voltage and current are low. Consequently, some researches tried to solve this problem by using average current mode control [14], series diode [15], adaptive look-up table on-time control [16], and variable on-time control [17]. Some researchers scrutinized different features of valley switching in LED drivers. In [18], the effect of reverse recovery of internal diode in metal-oxider-field-effect-transistor (MOSFET) is studied. In [19] the valley point is detected by current sense resistor's voltage instead of using a secondary winding coupled by converter inductance. In PFC boost converter, the input voltage changes from zero to peak voltage value since it is the rectified full bridge of main voltage. While the input current must follow the waveform of input voltage, the implementation of valley switching deteriorate the current waveform when the input voltage and current are low value. As a results, it increases THD. The effects of valley switching in Boost PFC converters have already been fully addressed [11]–[16]. On the other hand, for most of Buck LED drivers applications, in which both output voltage and current are at relatively high constant values, the valley switching is not a matter of concern. However, there are some applications of Buck LED drivers, such as dimming or thermal management, in which the output current is required to be low [20]–[24]. Upon these conditions, valley switching method malfunctions the performance of Buck LED drivers which are not addressed in the previous literatures. This paper studies the effect of valley switching in output current in Buck LED drivers and also a new method is proposed to solve its adverse effects. In general, the contributions of presented paper can be summarized as follow:

1) Elaborating the effect of valley switching in output current in Buck LED drivers when the output current intended to be low.

2) Proposing a new method namely semi valley switching to attenuate the adverse effects of valley switching which is validated with an experimental prototype.
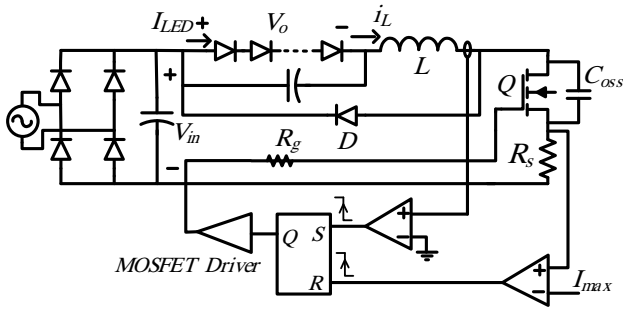
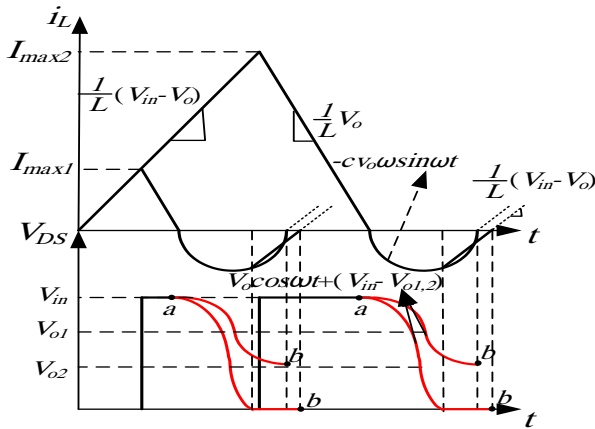Fig. 1: Buck LED driver in current control and valley switching mode.

Fig. 2: inductance current and MOSFET drain to source voltage.

II. VALLEY SWITCHING EFFECT IN BUCK LED DRIVER IN CURRENT CONTROL MODE

Fig. 1 shows the buck converter as a LED driver in current control and valley switching mode. Inductor current rises when switch Q turns on and it falls through diode when the switch turns off. The switch will turn on just the current reach zero to work in the border of CCM and DCM modes. In this case, the switching losses decrease because of zero current switching (ZCS). The other part of losses is occurred due to output capacitance of switch (C_{oss}) in spite of ZCS. When the diode is conducted, the output capacitance's voltage will reach to input voltage (V_{in}), therefore by turning the switch on, it will be discharged through the switch and it will result in another loss. Valley switching (VS) is used to prevent or attenuate these losses. As illustrated in Fig. 2, this capacitance will resonate through the inductor just the diode turns off. When its voltage reaches to its minimum value, the switch will turn on, and the losses will be minimized, consequently. For this purpose, as the inductor current is sensed to find the minimum value of voltage because when it reaches zero, the voltage reaches its minimum value (point b).

According to the Fig. 1, and assuming zero resistance for the simplicity of the analysis, the switch output capacitor (C_{oss}) voltage is as follows:
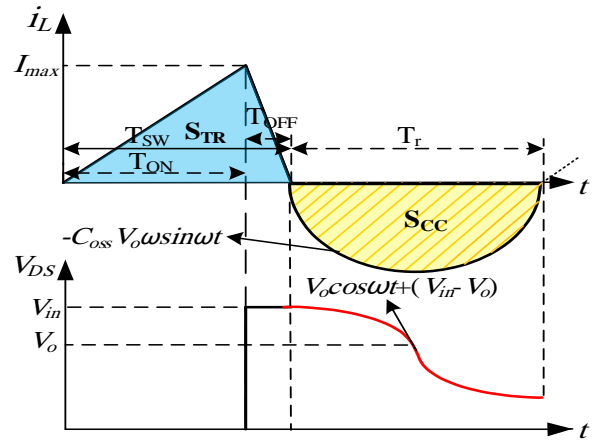

Fig. 3: Valley switching when V_{in} is greater than $2V_o$.

$$v_c(t) = V_o \cos \omega t + (V_{in} - V_o), \omega = \frac{1}{\sqrt{LC_{oss}}} \quad (1)$$

The inductor current is changed according to the reference maximum current (I_{max}). LED current is equal to its average values if the valley switching is not activated.

$$I_{LED} = \langle i_L \rangle = \frac{1}{2} I_{\max} \quad (2)$$

The inductor current is shown in Fig. 2 where the valley switching is implemented. Two cases can occur according to the input and output voltage values. When the input voltage (V_{in}) is greater than $2V_o$, a complete half resonance will occur according to (1). Fig. 3 shows this case where the inductor current is as (3).

$$i_L(t) = -C_{oss} V_o \omega \sin (\omega t) \quad (3)$$

Thus, the LED current can be achieved as:

$$I_{LED} = \langle i_L \rangle = f_{swcr} \times (\mathbf{S_{TR}} - \mathbf{S_{CC}}) \\ , \ f_{swcr} = \frac{1}{\mathrm{T_{sw}} + \mathrm{T_r}} \quad (4)$$

$$\mathbf{S_{TR}} = \frac{1}{2} I_{\max} \mathrm{T_{sw}} \ , \ \mathrm{T_{sw}} = \frac{L I_{\max} V_{in}}{V_o (V_{in} - V_o)} \quad (5)$$
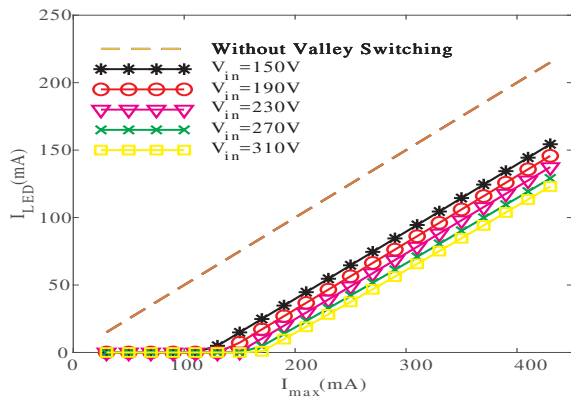
$$\mathbf{S_C} = 2C_{oss} V_o, T_r = \pi \sqrt{LC_{oss}} \quad (6)$$

The other case will occur when the input voltage (V_{in}) is smaller than $2V_o$. Fig. 4 shows this case. As shown the capacitor voltage reaches zero (point c) and is intended to be negative, but at this moment, the body diode of MOSFET is switched on and the inductor current will rise to zero. In this point the next switching will appeared. The LED current can be written as:

$$I_{LED} = \langle i_L \rangle = f_{swir} \times (\mathbf{S_{TR}} - \mathbf{S_{CI}} - \mathbf{S_{TRm}}) \\ , \ f_{swir} = \frac{1}{\mathrm{T_{sw}} + \mathrm{T_h} + \mathrm{T_{TRm}}} \quad (7)$$

$$\mathbf{S_{CI}} = C_{oss} V_{in}, \mathrm{T_h} = \frac{1}{\omega} \arccos \left(\frac{V_o - V_{in}}{V_o} \right) \quad (8)$$
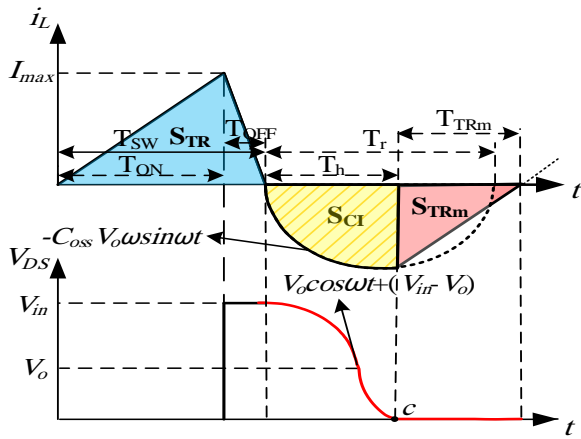
Fig. 4: Valley switching when V_{in} is lower than $2V_o$.

Fig. 5: I_{LED} for L=1000uH, C_{oss}=800pF and V_o=100V.

Fig. 6: Switching frequency for L=1000uH, C_{oss}=800pF and V_o=100V.

Fig. 7: Valley switching together with frequency limitation.

$$\mathbf{S_{TRm}} = C_{oss} \frac{2V_o V_{in} - V_{in}^2}{2\left(V_{in} - V_o\right)}, \mathbf{T_{TRm}} = \frac{\sqrt{2V_o V_{in} - V_{in}^2}}{\omega\left(V_{in} - V_o\right)} \quad (9)$$

Equation (4) and (7) indicate that the LED current is smaller when valley switching is activated in compared with the LED current when valley switching is not performed i.e. (2). Fig. 5 shows the LED current versus reference maximum current (I_{max}) for different input voltage values. It can be seen that the LED current will be zero if the reference maximum current is less than a limit at each input voltage value. In practical application, the LED starts to blink at this range because the output capacitor is discharged through LED and is charged again by the input voltage. In addition to zero current, there is a constant difference between the reference current and the actual current at each input voltage value therefore open loop current control is not sufficient to control current, accurately.

Equation (4) and (7) indicate that the frequency increases as the reference maximum current decreases. Fig. 6 illustrates a typical example of frequency changes as a function of reference maximum current at different input voltage values.

When the switching frequency is higher than a predetermined value, it is kept constant to limit the losses in an acceptable range. Fig. 7 shows the current and voltage waveform when the frequency reaches its maximum value. This figure is drawn when the input voltage (V_{in}) is smaller
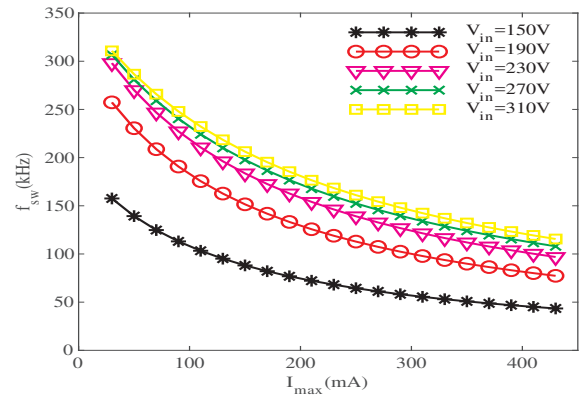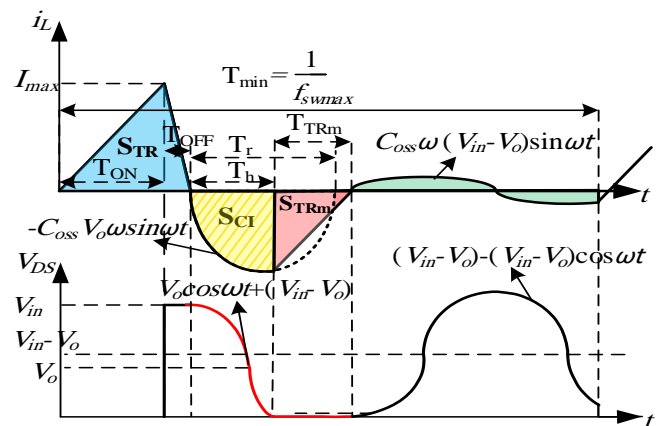
than $2V_o$ as example.

The capacitor voltage and inductor current equations are:

$$v_C(t) = (V_{in} - V_o) - (V_{in} - V_o)\cos\omega t \quad (10)$$

$$i_L(t) = C_{oss}(V_{in} - V_o)\,\omega\sin\omega t \quad (11)$$

As seen in (11), the current magnitude is proportional to (V_{in}-V_o). Thus, in compared with negative current magnetite in (3) which is proportional to V_o, it can be negligible when the difference between the input and output voltage is not a large value. When the frequency in higher than maximum switching frequency (f_{swmax}), the LED current is:

$$I_{LED} = \langle i_L \rangle = f_{sw\,max} \times (\mathbf{S_{TR}} - \mathbf{S_C} - \mathbf{S_{TRm}}) \quad (12)$$

Fig. 8 shows the LED current versus reference maximum current at different input voltage values when the maximum frequency is limited.

Comparing Fig. 5 and Fig. 8 shows that the zero current exists no matter frequency limitation is implemented or not. Also, for each input voltage, difference between the LED current and its reference maximum value is not constant when frequency limitation is applied.
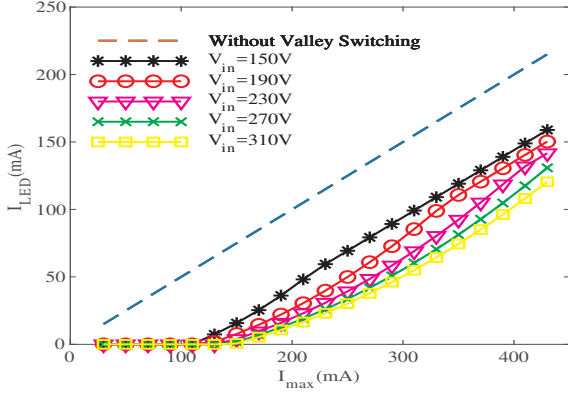
Fig. 8: I_{LED} for L=1000uH, C_{oss}=800pF, V_o=100V and f_{swmax}=100kHz.
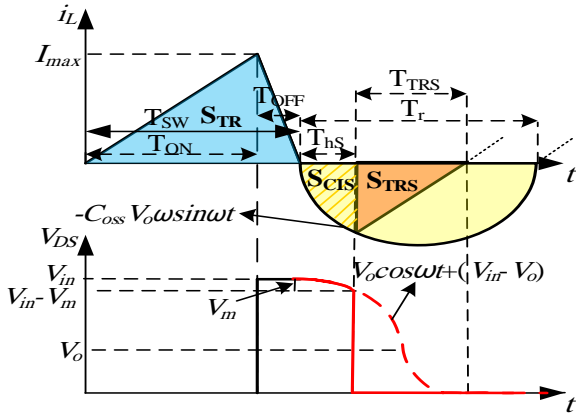

Fig. 9: Inductor current and MOSFET output voltage in semi valley switching.

III. SEMI VALLEY SWITCHING

As shown in the previous section when the reference maximum current decreases for dimming, it can cause the LED current falls to zero. The reason is shown in Fig. 3 and Fig. 4. Due to valley switching, a negative current flows through the inductor so its average current decreases. On the other hand, valley switching causes error between the reference maximum current and LED current. To avoid this problem, MOSFET must be in on-state between the moments when the diode goes OFF and before reaching minimum point of switch's output voltage. Under this condition, the switching loss increases, so a tradeoff between rising power losses and minimum current for dimming must be considered. Power losses depend on capacitor voltage values. It means that switching power losses drop when the MOSFET capacitor voltage decreases and also the LED current drops till it reaches zero so the current control is lost. Suppose the MOSFET turns on when its capacitor voltage falls to V_{in}-V_m value instead of valley point. Fig. 9 shows inductor current and MOSFET output voltage waveforms in this circumstance.

The on-state of switch occurs at T_h moment.

$$V_{in} - v_C(T_h) = V_m \tag{13}$$

$$T_h = \frac{1}{\omega} \arccos\left(\frac{V_o - V_m}{V_o}\right) \tag{14}$$

As shown in Fig. 9, the negative areas (S_{CIS}, S_{TRS}) are decreased by decreasing Vm but the switching losses increases and vice versa. Therefore, the dimming range or thermal management can be controlled to zero by adjusting the V_m proportional to the reference current. The average current is calculated as follows.

$$I_{LED} = \langle i_L \rangle = f_{swsv} \times (S_{TR} - S_{CIS} - S_{TRS})$$
$$, \quad f_{swsv} = \frac{1}{T_{sw} + T_{hS} + T_{TRS}} \tag{15}$$

$$S_{CIS} = C_{oss}V_m, T_{hS} = \frac{1}{\omega} \arccos\left(\frac{V_o - V_m}{V_o}\right) \tag{16}$$

$$S_{TRS} = C_{oss} \frac{2V_oV_m - V_m^2}{2(V_{in} - V_o)}, T_{TRS} = \frac{\sqrt{2V_oV_m - V_m^2}}{\omega(V_{in} - V_o)} \tag{17}$$

Fig. 10 shows the LED current versus the reference current at different input voltage values. V_m is increased from 0 to 100 volts proportional to reference maximum current. Upon these conditions, the switch losses consist of conducting losses and on-state switching losses can be managed. It means that when the reference maximum current decreases the conducing losses of switch decreases whereas the on-state switching losses increases and vice versa.

Comparing Fig. 8 and Fig. 10b shows that the zero LED current does not appear when the new method is implemented in spite of voltage variation. The main switch losses can be divided in two parts of switching and conduction losses. The switching losses increases as the valley switching is not implemented. Working at the margin of CCM and DCM modes causes ZCS switching. Therefore, the on-switching losses does not exist for this case.

$$P_{sw} = \frac{f_{sw}}{2}\left(I_{max}V_{in}t_{OFF} + C_{oss}V_{in}^2\right), f_{sw} = \frac{1}{T_{sw}} \tag{18}$$

where t_{OFF} is turn-off time of MOSFET. Switching losses are changed if the valley switching is applied. They are different according to the input and output voltage values.

$$P_{sw} = \begin{cases} \frac{f_{swcr}}{2}\left(m + C_{oss}(V_{in} - 2V_o)^2\right)V_{in} \geq 2V_o \\ \frac{f_{swir}}{2}m, m = I_{max}V_{in}t_{OFF} \quad V_{in} < 2V_o \end{cases} \tag{19}$$

The switching losses depend on Vm in the case of semi valley switching.
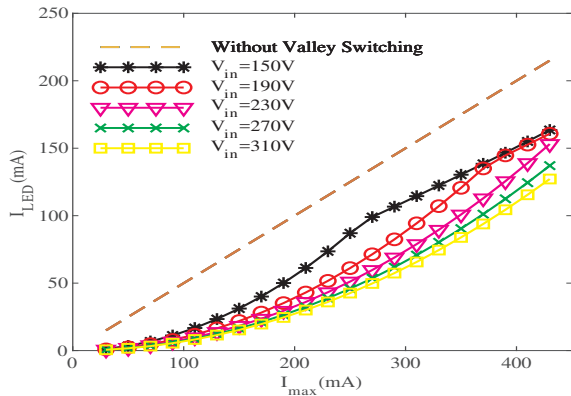
$$P_{sw} = \frac{f_{sws}}{2}\left(I_{max}V_{in}t_{OFF} + C_{oss}(V_{in} - V_m)^2\right) \tag{20}$$

The conducting losses are determined by rms value of conducting current and on-state resistance of MOSFET (R_{ON}), therefore they depend on reference maximum current when the valley switching is not performed.

$$P_{cond} = R_{ON}\frac{I_{max}^2}{3}T_{ON}f_{sw} \tag{21}$$
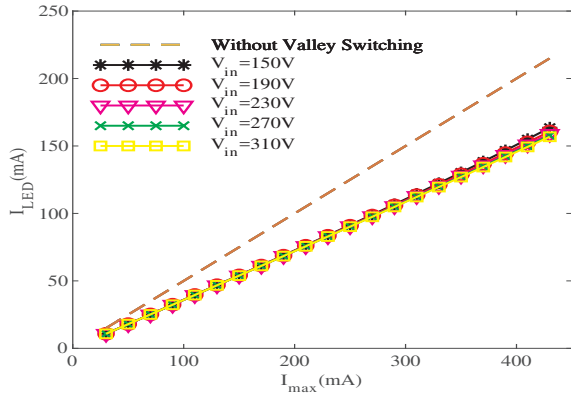
(a) Without frequency limitation.

(b) With frequency limitation (f_{swmax}=100kHz).

Fig. 10: I_{LED} using semi valley switching for L=1000uH, C_{oss}=800pF and V_o=100V.

(a) Switching losses.

(b) Conduction losses.

Fig. 11: Switching and conducting losses of MOSFET for R_{DS}=4.5 Ω, t_{OFF}=160ns and f_{swmax}=100kHz.

Similar to switching losses, the conducting losses depend on input and output voltage values as follows.

$$P_{cond} = \begin{cases} R_{ON}\dfrac{I_{\max^2}}{3}T_{ON}f_{swcr} & V_{in} \geq 2V_o \\ R_{ON}\dfrac{I_{\max^2}}{3}T_{ON}f_{swir} & V_{in} < 2V_o \end{cases} \quad (22)$$
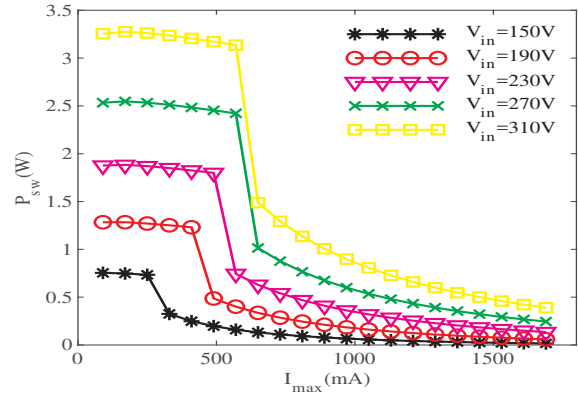
In semi valley switching, it can be represented as:

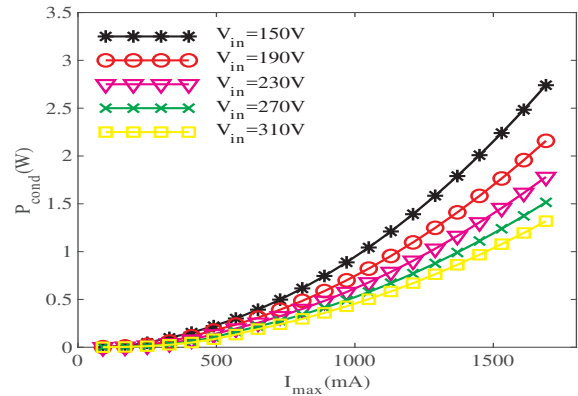$$P_{cond} = R_{ON}\frac{I_{\max^2}}{3}T_{ON}f_{swsv} \quad (23)$$

Note that, if the frequency limitation is activated, Switching and conducting losses will decrease. As an example, the conducting loss in (23) will be:

$$P_{cond} = \begin{cases} R_{ON}\dfrac{I_{\max^2}}{3}\mathrm{T_{ON}}f_{swir} & f_{swir} \leq f_{sw\,\max} \\ R_{ON}\dfrac{I_{\max^2}}{3}\mathrm{T_{ON}}f_{sw\,\max} & f_{swir} > f_{sw\,\max} \end{cases} \quad (24)$$
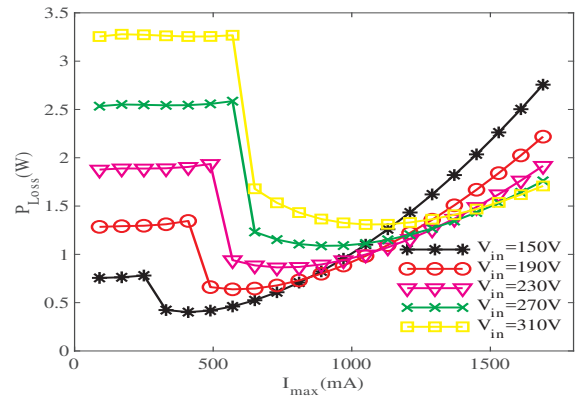
Fig. 11 shows the switching and conducting losses for semi valley switching and Fig. 12 shows the sum of switching and conducting losses. As seen, when the switching losses increases, the conducting losses will decrease; therefore the total losses of the switch will remain in acceptable range. Although

Fig. 12: Sum of switching and conducting losses of MOSFET R_{DS}= 4.5 Ω and t_{OFF}=160ns.

the efficiency will decrease if complete valley switching is not done, it deteriorates the LED current and diminishes it to zero in low current range.

Implementation of this method can be simple for either dimming or thermal management purposes. Many converters switching ICs have synchronizing capability that can be used to implement the new method. For example, UC3842/3/4/5 ICs can do this function using oscillator pin and an external clock.
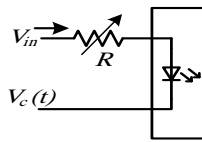
Fig. 13: Using a high speed optocoupler to implement the semi valley switching.

Fig. 13 shows the implementation of semi valley switching using an optocoupler that should be connected to synchronizing pin of switching IC. This configuration can detect the zero current of diode and implement the (13). Voltage across input pins of optocoupler is equal to forward voltage of converter diode when it is conducting; therefore it is in off-state. When the diode turns off and the output voltage of C_{oss} falls lower than required value to turn on the optocoupler, it turns on and enables the UC3844. In this configuration, the V_m can be adjusted by resistance value (R) or a NTC resistance can be used in thermal management application. Assume that the minimum value of optocoupler forward current is I_{min}; therefore V_m is as follows.

$$V_m = R I_{\min} \tag{25}$$

The optocoupler produces a rising edge pulse to turn on the switch when the difference between the input and output voltages reaches to the limit value (V_m).

In a lot of LED lamps, a thermal management is implemented. It means that the LED current decreases when temperature reaches a predetermined valued. In this application, a NTC can be used instead of R. As temperature rises, the reference maximum current drops to decrease the temperature. On the other hand, the NTC resistance and consequently limit value (V_m) decreases; therefore, working in lower current will be possible.

IV. EXPERIMENTAL RESULTS

Fig. 14 shows the experimental setup for buck LED driver. A 40W/100V LED lamp is used as a load and UC3844 is used in current control and synchronizing mode. A potentiometer (R_{pc}) and an autotransformer are used to change the reference maximum current and the input voltage, respectively. Semi valley switching is implemented using the method mentioned in the previous section. A $1.2\,\Omega$ resistance is connected between source pin of MOSFET and ground and its voltage is used for current sense of IC after passing through a low-pass RC filter. Fig. 15 shows the inductance current, and LED current in conditions of input voltage (V_{in}) greater than $2V_o$. While Vin is equal to 250 Volts, the reference maximum currents are 400mA and 100mA for subfigures (a) and (b), respectively. As seen in Fig. 15, a complete half cycle of resonance occurs and its effect is predominant when the inductance current is low (Fig. 15b). As shown in Fig. 3 and (6), the negative area related to the resonance current depends on output voltage instead of current; therefore it is constant in high or low reference maximum current of inductance (Fig. 15a and Fig. 15b). This causes its effect is more predominant when
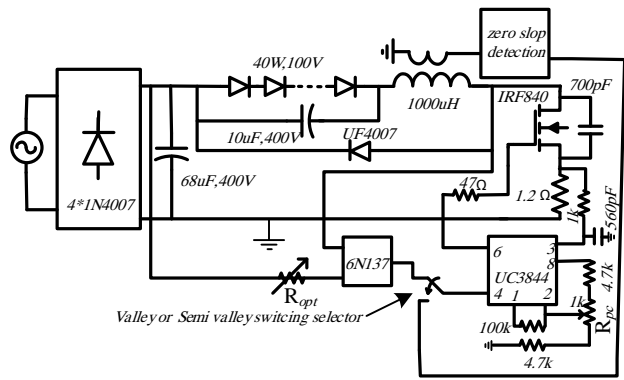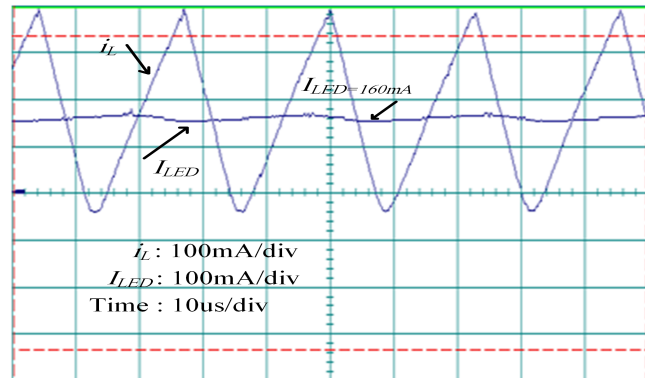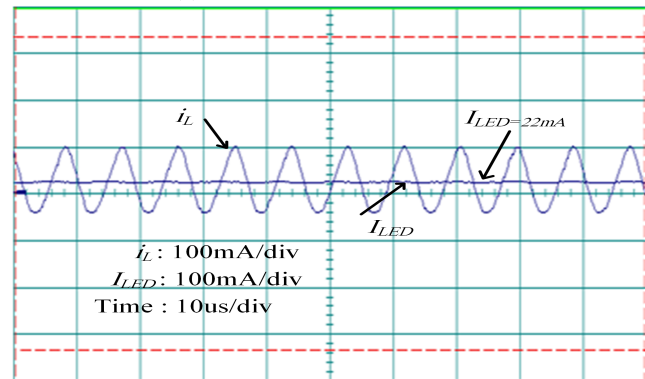

Fig. 14: Experimental semi and full valley switching circuit.

(a) i_L and I_{LED} for I_{max}=400mA.

(b) i_L and I_{LED} for I_{max}=100mA.

Fig. 15: Inductance and LED currents for I_{max}=100mA, I_{max}=400mA and V_{in}=250V.

the reference maximum current is low. The LED current is around 160mA when the reference current is 400mA. Without valley switching and according to (2), it should be 200mA. The proportion is 0.8 while this value for 100mA reference maximum current is 0.44 which shows the adverse effect of valley switching is worsen in low current.

Fig. 16 shows the inductance and LED current in conditions when the input voltage (V_{in}) is lower than $2V_o$. The reference maximum current is adjusted to 400mA and 100mA similar to the previous experiment. As illustrated in Fig. 4 and (7), the negative area is not a complete half cycle but like the previous
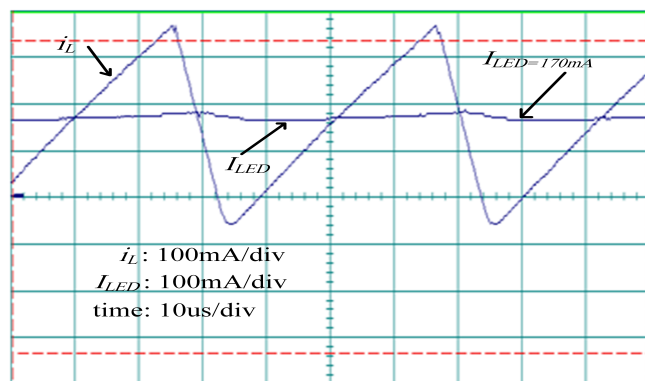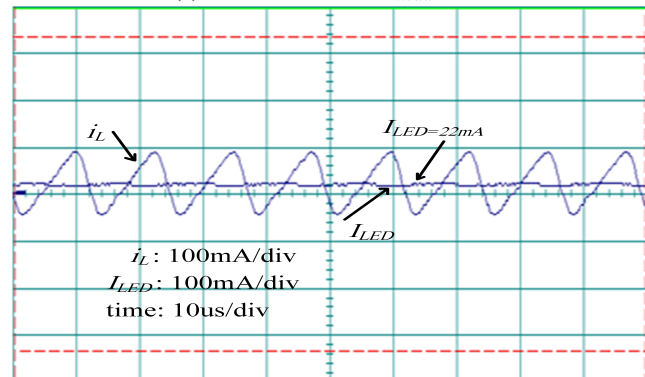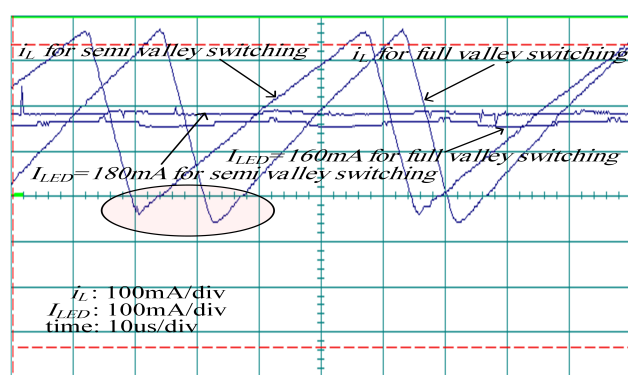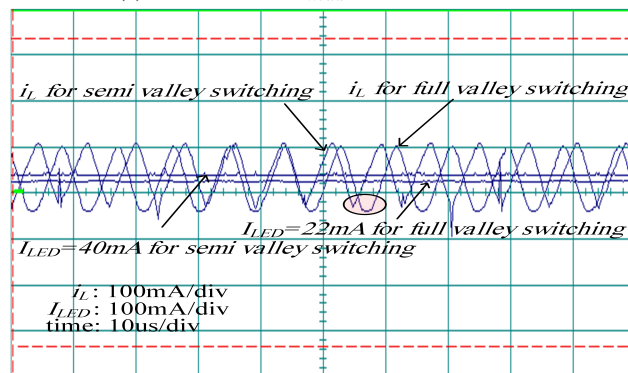
(a) i_L and I_{LED} for I_{max}=400mA.

(a) i_L current for I_{max}=400mA.

(b) i_L and I_{LED} for I_{max}=100mA.

(b) i_L current for I_{max}=100mA.

Fig. 16: Inductance and LED current for I_{max}=100mA, I_{max}=400mA and V_{in}=150V.

Fig. 17: Comparison on inductance and LED current for 100mA and 400mA reference maximum current.

case its effect is predominant in low current (Fig. 16b).

The same reference maximum current values are used in semi valley switching to evaluate and compare it with full valley switching. Fig. 17 shows the inductance current in low and high values (400mA reference maximum current for high current and 100mA reference maximum current for low current), when the input voltage is lower and greater than $2V_o$ (Fig. 17a for V_{in}=150V and Fig. 17b for V_{in}=250V) to compare the operation of the full valley and semi valley switching methods. As shown in Fig. 3, Fig. 4 and Fig. 9, the negative area in semi valley switching is lower than the full valley switching. This area can be changed by adjusting the resistance value of optocoupler resistor (R_{opt}). Also, the LED current for both cases are shown in Fig. 17. As expected, the LED current in semi valley control is higher than the full valley control. The ratios of LED current to its value calculated using (2) for low and high current are 0.8 and 0.9, respectively. Comparing these values with their similar cases achieved in the previous experiments proved the effectiveness of the semi valley switching.

The switching frequency rises when the maximum reference current increases. This problem is shown in Fig. 6. The switching ICs keep the on-time or off-time in constant values or define a limitation value for them to implement the maximum switching frequency (F_{swmax}). At this situation, as illustrated in Fig. 7 and (10)-(12), if output voltage is not significantly smaller than the input voltage, the LED current

treats similar to condition that the frequency limitation is not performed because the oscillation current amplitude is significantly smaller that its peak minus value. A new circuit is designed to show the effect of frequency limitation. This buck LED driver works in current control mode similar to the first LED diver, but at fixed frequency. The designed circuit works in DCM mode when the current is lower than a critical value. Fig. 18 illustrates the operation of the circuit at the case. As seen, the negative area and its effect is like to the previous figures. When the drain to source voltage is about to negative value, the body diode of MOSFET turns on and clamps it to zero. Upon this condition, the inductance current will rise to zero. When the inductance current reaches to zero, the diode turns off and another resonance circuit is occurred between inductance and MOSFET output capacitance. Equation (10) shows the MOSFET output voltage. Note that it never becomes negative, therefore the diode does not turns on.

V. CONCLUSION

In spite of high performance of valley switching in decreasing the switching losses, it has adverse effects on the performance of the Buck LED driver when decreasing the LED current is required for dimming, thermal management, or precise current adjustment applications. The reason is that it causes to flow negative output current through the converter inductance which decreases the LED current. The valley
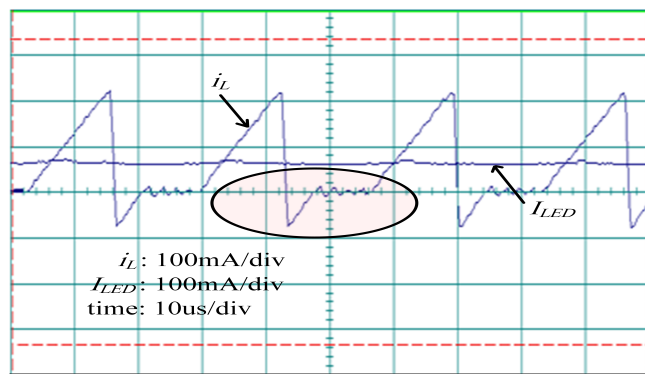
Fig. 18: Frequency limitation effect on LED current.

switching causes zero output current when the reference maximum current (I_{max}) is low, therefore the LED current does not react the change of reference maximum current in low current range. Regarding this malfunction of valley switching in low current, a semi valley switching is introduced in this study. In the proposed method, the switching is applied at a moment between zero current of converter diode and next valley point of drain to source voltage. It can be implemented when the current and the conducting losses is low; therefore, almost the equivalent losses remain constant. The proposed methodology, which is validated with an experimental prototype, indicates the high performance of semi valley switching in different applications of LED drivers with a range of low to high output current.

References

[1] J. Baek and S. Chae, "Single-stage buck-derived led driver with improved efficiency and power factor using current path control switches," *IEEE Transaction on Industrial Electronics*, vol. 64, DOI 10/1109/TIE.2017.2698404, no. 10, pp. 7852–7861, Oct. 2017.

[2] Y. C. Liu, F. C. Syu, H. C. Hsieh, K. A. Kim, and H. J. Chiu, "Hybrid switched-inductor buck pfc converter for high-efficiency led drivers," *IEEE Transactions on Circuits and Systems II*, vol. 65, DOI 10/1109/TCSII.2017.2787554, no. 8, pp. 1069–1073, Aug. 2017.

[3] F. Wang, L. Li, Y. Zhong, and X. Shu, "Flyback-based three-port topologies for electrolytic capacitor-less led drivers," *IEEE Transactions on Industrial Electronics*, vol. 64, DOI 10/1109/TIE.2017.2677303, no. 7, pp. 5818 – 5827, Jul. 2017.

[4] J. LIU, H. TIAN, G. Liang, J. ZENG, and J. ZENG, "A bridgeless electrolytic capacitor-free led driver based on series-resonant converter with constant frequency control," *IEEE Transaction on Power Electronics*, vol. 34, DOI 10/1109/TPEL.2018.2847701, no. 3, pp. 2712–2725, Mar. 2019.

[5] R. A. Sangrody, J. Nazarzadeh, and K. Y. Nikravesh, "Bifurcation and lyapunov's exponents characteristics of electrical scalar drive systems," *IET Power Electronics*, vol. 5, DOI 10/1049/iet-pel.2011.0024, no. 7, pp. 1236–1244, Aug. 2012.

[6] R. A. Sangrody, J. Nazarzadeh, and K. Y. Nikravesh, "Inherent chaotic behavior in vector control drives of induction machines," *Electric Power Components and Systems*, vol. 40, DOI 10/1080/15325008.2011.621509, no. 1, pp. 1–20, Nov. 2011.

[7] G. Z. Abdelmessih, J. M. Alonso, and M. A. D. Costa, "Loss analysis for efficiency improvement of the integrated buck-flyback led driver," *IEEE Transactions on Industry Applications*, vol. 65, DOI 10/1109/TIA.2018.2858739, no. 6, pp. 6543–6553, Nov. 2018.

[8] Y. Wang, X. Hu, Y. Guan, and D. Xu, "A single-stage led driver based on half bridge clcl resonant converter and buck-boost circuit," *IEEE Journal of Emerging and Selected Topics in Power Electronics*, vol. 7, DOI 10/1109/JESTPE.2018.2861740, no. 1, pp. 196–208, Mar. 2019.

[9] J. M. Wang and S. T. Wu, "A synchronous buck dc-dc converter using a novel dual-mode control scheme to improve efficiency," *IEEE Transactions on Power Electronics*, vol. 32, DOI 10/1109/TPEL.2016.2623353, no. 9, pp. 6983–6993, Sep. 2017.

[10] S. W. Lee and H. L. Do, "Single-stage bridgeless ac-dc pfc converter using a lossless passive snubber and valley switching," *IEEE Transactions on Industrial Electronics*, vol. 63, DOI 10/1109/TIE.2016.2577622, no. 10, pp. 6055–6063, Oct. 2016.

[11] C. J. H. Nene and S. Choudhury, "Efficiency and thd optimization based on an interleaved pfc converter using digital controller with integrated valley switching control feature," in *IEEE Texas Power and Energy Conference (TPEC)*, DOI 10/1109/TPEC.2019.8662175, pp. 1–5, Feb. 2019.

[12] H. Nene, C. Jiang, and S. Choudhury, "Digital controller with integrated valley switching control for light load efficiency and thd improvements in pfc converter," in *IEEE Applied Power Electronics Conference and Exposition (APEC)*, DOI 10/1109/APEC.2017.7930940, pp. 1785–1788, Mar. 2017.

[13] L. Huber, B. T. Irving, and M. M. Jovanovic, "Effect of valley switching and switching-frequency limitation on line-current distortions of dcm/ccm boundary boost pfc converters," *IEEE Transactions on Power Electronics*, vol. 24, DOI 10/1109/TPEL.2008.2006053, no. 2, pp. 339–347, Feb. 2009.

[14] R. T. Ryan, J. G. Hayes, R. J. Morrison, and D. N. Hogan, "Improved zero-crossing distortion of a boundary-conduction-mode boost converter with digital average-current-mode control," in *IEEE Applied Power Electronics Conference and Exposition (APEC)*, DOI 10/1109/APEC.2018.8341268, pp. 1846–1853, Mar. 2018.

[15] Q. Li, K. Yao, J. Song, H. Xu, and Y. Han, "A series diode method of suppressing parasitic oscillation for boost pfc converter operated in discontinuous conduction mode," *IEEE Transactions on Power Electronics*, vol. 33, DOI 10/1109/TPEL.2017.2668605, no. 1, pp. 407–424, Jan. 2018.

[16] X. Ren, Z. Guo, Y. Wu, Z. Zhang, and Q. Chen, "Adaptive lut-based variable on-time control for crm boost pfc converters," *IEEE Transactions on Power Electronics*, vol. 33, DOI 10/1109/TPEL.2017.2772313, no. 9, pp. 8123–8136, Sep. 2018.

[17] Y. Zhou, X. Ren, Z. Guo, Z. Zhang, Q. Chen, and K. Yao, "A more accurate variable on-time control for crm flyback pfc converters," in *IEEE Energy Conversion Congress and Exposition (ECCE)*, DOI 10/1109/ECCE.2018.8557689, pp. 1–6, Sep. 2018.

[18] C. Zhao and X. Wu, "Accurate operating analysis of boundary mode totem-pole boost pfc converter considering the reverse recovery of mosfet," *IEEE Transactions on Power Electronics*, vol. 33, DOI 10/1109/TPEL.2018.2829832, no. 12, pp. 10 013–10 043, Dec. 2018.

[19] Y. G. Li, "A novel control scheme of quasi-resonant valley-switching for high-power-factor ac-to-dc led driver," *IEEE Transactions on Industrial Electronics*, vol. 62, DOI 10/1109/TIE.2015.2397875, no. 8, pp. 4787–4794, Aug. 2015.

[20] P. Y. Lin, T. J. Liang, C. W. Chang, K. H. Chen, and B.-K. Huang, "Buck-type wide-range dimmable led driver," in *IEEE Applied Power Electronics Conference and Exposition (APEC)*, DOI 10/1109/APEC.2017.7930907, pp. 1563–1569, Mar. 2017.

[21] T. N. Gucin, B. Fincan, and M. Biberoglu, "A series resonant converter based multi-channel led driver with inherent current balancing and dimming capability," *IEEE Transactions on Power Electronics*, vol. 34, DOI 10/1109/TPEL.2018.2838261, no. 3, pp. 2693–2703, Mar. 2019.

[22] M. Taha and T. Hu, "Multiple string led driver with flexible and high performance pwm dimming control," *IEEE Transactions on Power Electronics*, vol. 32, DOI 10/1109/TPEL.2017.2655884, no. 12, pp. 9293–9306, Dec. 2017.

[23] S. Li, Y. Guo, S.-C. Tan, and S. Y. R. Hui, "An off-line single-inductor multiple-outputs led driver with high dimming precision and full dimming range," *IEEE Transactions on Power Electronics*, vol. 32, DOI 10/1109/TPEL.2016.2597237, no. 6, pp. 4716–4727, Jun. 2017.

[24] S. C. Hsia, M. H. Sheu, J. J. Jhou, and S. Y. Lai, "Embedded temperature sensor for multilevel current led driver," *IEEE Sensors Journal*, vol. 14, DOI 10/1109/JSEN.2014.2316284, no. 8, pp. 2801–2806, Aug. 2014.